

Study of scintillation in natural and synthetic quartz and methacrylate

J. Amaré, S. Borjabad, S. Cebrián¹, C. Cuesta², D. Fortuño³, E. García, C. Ginestra, H. Gómez⁴, D.C. Herrera, M. Martínez, M.A. Oliván, Y. Ortigoza, A. Ortiz de Solórzano, C. Pobes⁵, J. Puimedón, M.L. Sarsa, J.A. Villar and P. Villar

*Laboratorio de Física Nuclear y Astropartículas, Universidad de Zaragoza
Calle Pedro Cerbuna 12, 50009 Zaragoza, Spain
Laboratorio Subterráneo de Canfranc
Paseo de los Ayerbe s/n, 22880 Canfranc Estación, Huesca, Spain*

Abstract

Samples from different materials typically used as optical windows or light guides in scintillation detectors were studied in a very low background environment, at the Canfranc Underground Laboratory, searching for scintillation. A positive result can be confirmed for natural quartz: two distinct scintillation components have been identified, not being excited by an external gamma source. Although similar effect has not been observed neither for synthetic quartz nor for methacrylate, a fast light emission excited by intense gamma flux is evidenced for all the samples in our measurements. These results could affect the use of these materials in low energy applications of scintillation detectors requiring low radioactive background conditions, as they entail a source of background.

Keywords: quartz, methacrylate, scintillation, low radioactive background
PACS: 42.70.Ce, 29.40.Mc, 21.10.Tg,

1. Introduction

Scintillation detectors are used, among many other applications, in rare event searches as the study of the neutrinoless double beta decay [1] or the direct detection of hypothetical dark matter particles pervading our galactic halo [2].

¹Corresponding author

²Present address: Center for Experimental Physics and Astrophysics, University of Washington, Seattle, WA, US

³Present address: ENDESA Generación, Lleida, Spain

⁴Present address: Laboratoire de l'Accélérateur Linéaire (LAL). Centre Scientifique d'Orsay. Bâtiment 200 - BP 34. 91898 Orsay Cedex, France.

⁵Present address: Instituto de Ciencia de Materiales de Aragón, Universidad de Zaragoza - CSIC

Improving the background levels and energy thresholds of scintillation detectors is still a challenging issue. Photomultiplier Tubes (PMTs) were typically a strong background source, however, ultra-low background models are becoming state of the art, and then, other contributions to the background become more relevant [3, 4]. In the case of inorganic scintillators, being NaI(Tl) one with the most outstanding performance, PMTs are typically coupled to the scintillator crystal through light guides or optical windows made of different materials, whose design is based on geometry or background considerations. In the development of prototypes for the ANAIS (Annual modulation with NaI Scintillators) experiment [5] operating in the Canfranc Underground Laboratory (LSC, Laboratorio Subterráneo de Canfranc, Spain) and using NaI(Tl) crystals as target material, understanding of the different background contributions has been a major issue: residual radioactive backgrounds have been studied in [6], a very slow scintillation time constant in NaI(Tl) able to trigger the experiment and then, contribute to the background, was identified recently [7], and the results of the scintillation study of different materials considered to be used as optical windows and light guides are presented in this letter. This study was motivated by the identification, in previous ANAIS prototype tests using natural quartz optical windows, of a population of events, which contributed to the background at very low energy, and whose pulses showed an abnormal temporal behavior, since their decay was faster than expected for NaI(Tl) scintillation events. This letter describes a specific mounting and the set of measurements carried out in order to confirm and characterize a possible scintillation in natural quartz, and to test, under similar conditions, other suitable materials for the same purpose, namely synthetic quartz and methacrylate, to be sure that a similar effect is not present and they could be used in dark matter experiments. This study is not directly related with the dark matter search goal of ANAIS experiment, in whose context natural quartz was directly discarded as optical window because of the high radioactive content of the material. However, scintillation in natural quartz had not been previously related with fast populations of events in NaI(Tl) detectors, and in our opinion, this issue deserved more understanding.

Events produced by a weak scintillation in the materials searched for would appear entangled with dark events from PMTs, being difficult to discriminate. This PMT noise is mainly due to thermoionic electron emission, but other contributions can be present due, for instance, to the emission of Cherenkov light (generated by radioactive contamination in the PMT, in their neighborhood or, even, by the interaction of cosmic rays) and ions in residual gas inside the PMT [8]. Operating two PMTs in coincidence is a common and effective practice in experiments demanding a low energy threshold in order to diminish the contribution from the thermoionic effect. However, Cherenkov light emission can produce coincident events, although they are expected to be quite asymmetric. Residual gas ions typically produce afterpulses, not relevant for coincidence measurements. The residual noise when operating PMTs in coincidence, as it is done in this work, attributed to accidental coincidences from dark events and to the generation of light in one PMT being detected by the other, had been studied in [9].

Quartz is not considered as a scintillating material in the literature [10, 11]; a weak scintillation was reported under irradiation with α particles [10, 12], although it was not characterized. However, quartz is largely used for dosimetry and dating thanks to thermal and optically stimulated luminescence, since it can emit when heated or illuminated an amount of light proportional to the radiation dose accumulated in time [13]. Imperfections (impurities or defects) in crystalline materials (as quartz) disturb the periodicity of the crystalline electric field, generating dips in the electric potential where free electrons may be trapped (the so-called electron traps). Ionizing radiation is able to excite electrons into the conduction band, that eventually could fall in such traps. Hence, the amount of electrons trapped is proportional to the radiation dose received. In the case of materials used for dosimetry or dating, when the irradiated material is heated or exposed to strong light, trapped electrons can absorb enough energy to return into the conduction band and then, recombine with holes in the valence band emitting part of the energy in the form of luminescence. In the case of quartz, used for optical dating, green or blue light is used to free the trapped electrons and luminescence in the ultraviolet is produced and read out. Then, scintillation in the ultraviolet range is expected from quartz also directly following energy deposition from ionizing radiation, in a time scale dependent on the lifetime of the radiative decaying states participating in the scintillation mechanism and with, probably, very low intensity. Characterization and understanding of such a scintillation was the main goal of this work.

In section 2 the experimental setup and the plan of measurements carried out to study possible scintillation in different quartz and methacrylate samples, to be used as optical windows and/or light guides with NaI(Tl) crystals, are described. Analysis performed and results obtained are presented in section 3, considering first the measurements made without sample and then those with the different samples. Section 4 gathers the conclusions.

2. Experimental set-up and summary of measurements

A test bench was conditioned at LSC to study scintillation from different samples. It consisted of two photomultipliers (Electron Tubes 9302B model, 3 inches diameter) faced at a fixed 10 cm distance between their respective photocathodes, in order to keep as much as possible the same geometry in the different measurements. The samples were placed centered in the inner space, between the PMTs (see figure 1), without using optical grease for the coupling to the PMTs to minimize the incorporation of unnecessary components that could affect the comparison between samples. Photomultipliers were operated at 1100 V. According to the 9302B series data sheet, the transit time is 40 ns and the single electron response (SER) rise time is 7.5 ns and 15 ns the corresponding FWHM. The nominal dark count rate at 20°C is 500 s⁻¹. The spectral response curve ranges from 300 to 500 nm, having the maximum at 350-400 nm. Charge readout of the PMT is fast enough to keep the single electron time behavior. Samples and PMTs were housed in a 0.1-mm-thick μ -metal lining, covered by a plastic container made of PVC to avoid environmental light reaching the PMTs.

Table 1: Main features of the samples studied in this work: material, supplier, dimensions and measured activities (or upper limits) of ^{232}Th and ^{238}U natural chains using HPGe spectrometry at LSC [6].

Material	Supplier	Diameter (mm)	Height (mm)	^{232}Th	^{238}U	^{40}K	units
Natural quartz (Homosil)	Heraeus	76.4	10	33 ± 4	228 ± 9	< 50	mBq/kg
Synthetic quartz (Suprasil 2 grade B)	Heraeus	76.2	10	< 4.7 ^{228}Ra < 2.5 ^{228}Th	< 100 ^{238}U < 1.9 ^{226}Ra	< 12	mBq/kg
Methacrylate (PMMA) ⁶	Goodfellow	78.0	100	< 4.5 ^{228}Ra < 5.0 ^{228}Th	< 120 ^{238}U < 4.7 ^{226}Ra	< 21	mBq/guide

Since the dark counting rate of PMTs can be affected by environmental gamma or cosmic ray fluxes, the set-up was operated in low background conditions: a 10-cm-thick lead shielding was used to reduce the contribution from environmental gamma radiation and all measurements were carried out at LSC, located in the Spanish Pyrenees, under a rock overburden of 2450 m.w.e. Underground operation at such a depth guarantees a significant cosmic ray suppression; the measured muon flux at LSC is of the order of $10^{-7} \text{ cm}^{-2}\text{s}^{-1}$ [14, 15], which means a reduction of about five orders of magnitude with respect to the flux above ground.

Three different samples have been studied in this test bench: natural and synthetic quartz and methacrylate. Synthetic and natural quartz samples are from Suprasil and Homosil series from Heraeus, respectively. According to supplier specifications, for Homosil quartz only carefully selected crystal is used as raw material; it has no particulate structure and extremely favorable homogeneity properties. Suprasil 2 is a high purity synthetic fused silica material manufactured by flame hydrolysis of SiCl_4 ; the index homogeneity is controlled and specified in one direction. Other relevant information about the samples is given in table 1; for quartz samples, two identical cylinders as those described in table 1 were placed together in the bench. The samples were screened for radiopurity at the LSC using an ultra-low background HPGe detector in order to determine the corresponding activity of the ^{232}Th and ^{238}U natural chains and ^{40}K [6]. Results are shown in table 1. For the natural quartz samples, data are compatible with equilibrium in both chains; for synthetic quartz and methacrylate, upper limits are given for ^{238}U , ^{226}Ra , and for the long-lived daughters of ^{232}Th .

Data acquisition directly ran at a Tektronix oscilloscope (Digital Phosphor Oscilloscope, TDS5034B) having 4 channels and a bandwidth of 350 MHz. Pulse shapes were digitized in a window of $2 \mu\text{s}$ taking 2500 samples. Trigger was done

⁶Screening of the methacrylate sample was carried out including also a copper can.

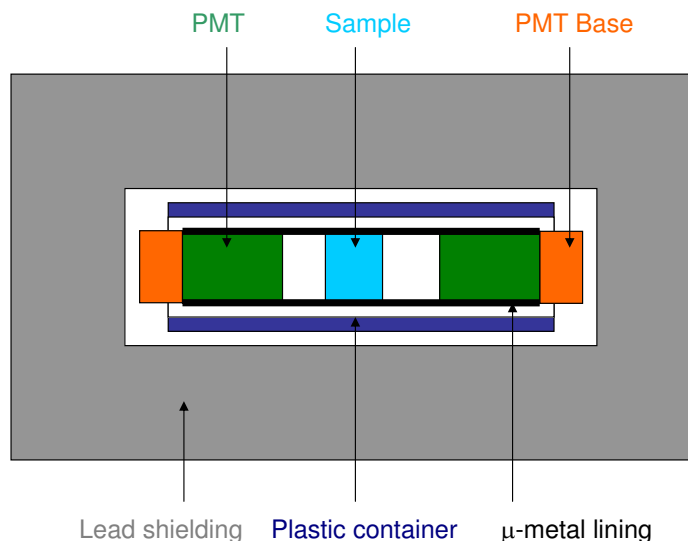


Figure 1: Sketch of the scintillation test bench used for the measurements presented in this work: a plastic cylinder houses the scintillator sample and two PMTs lined in μ -metal, inside a lead shielding at the Canfranc Underground Laboratory.

at photoelectron level in logical AND between the two PMT signals in order to reduce dark events. Time and the two digitized PMT pulses were recorded for each event; we will refer below to both digitized PMT signals as 0 and 1, respectively.

Table 2 summarizes all the measurements performed, including live time and trigger rates registered. For every sample, two measurements were carried out, without external excitation (we will refer to as background measurement) and under exposure to gamma radiation produced by an external ^{232}Th source with activity of ~ 5 kBq placed inside the shielding. Special measurements without sample were also made, both in background conditions and using the ^{232}Th source, and even using a black cardboard between the PMTs to suppress possible effects from light emission in a PMT generating a coincident event in the other one.

3. Analysis and Results

In a first analysis, a set of parameters was calculated for every registered event and saved in ROOT [16] files for further analysis. Among these parameters, we will use in the following:

- The area of the pulse.

Table 2: Summary of measurements performed in the scintillation test bench at LSC: sample type, exposure to an external gamma ^{232}Th source, live time and trigger rate.

Sample	External gamma source	Live time (h)	Trigger rate (h^{-1})
without sample	No	79.60	921.4 ± 3.4
natural quartz	No	319.11	1218.0 ± 2.0
synthetic quartz	No	314.41	940.4 ± 1.7
methacrylate	No	908.33	621.38 ± 0.83
without sample	Yes	0.52	$(12.79 \pm 0.16) \times 10^3$
natural quartz	Yes	0.83	$(79.69 \pm 0.31) \times 10^3$
synthetic quartz	Yes	2.08	$(70.74 \pm 0.19) \times 10^3$
methacrylate	Yes	2.30	$(149.78 \pm 0.26) \times 10^3$
without sample, black cardboard between PMTs	Yes	2.15	656 ± 17

- The so-called P1 defined as:

$$P1 = \frac{\text{Area}(100 - 600\text{ns})}{\text{Area}(0 - 600\text{ns})} \quad (1)$$

where the beginning of the pulse defines the zero time. This parameter has been successfully used to disentangle PMT origin events from real scintillation events at very low energy in NaI(Tl) detectors [5, 17], profiting from the quite long scintillation main time constant (~ 230 ns) vs typical PMT pulses FWHM⁷. P1 distribution for noise is centered at 0 while for NaI(Tl) scintillation events peaks typically at ~ 0.7 .

- The number n of peaks identified in the pulse. Profiting from the good sampling rate of the digitized data, the discrete arrival of the photons to the PMT photocathode can be distinguished in the pulses corresponding to low energy events. An algorithm that finds and counts the number of peaks in the pulse has been developed, it is based on the TSpectrum ROOT class and the Search method [18]. Peaks are considered gaussian with a minimum height and width, selected specifically according to the SER of the PMT used.
- The possible correlation of the light shared between the two PMT signals will be studied by evaluating the asymmetry parameter:

$$Asy = \frac{\text{Area}_{\text{signal0}} - \text{Area}_{\text{signal1}}}{\text{Area}_{\text{signal0}} + \text{Area}_{\text{signal1}}} \quad (2)$$

⁷The FWHM of the SER for PMT models used for individual photon counting are typically below 30 ns.

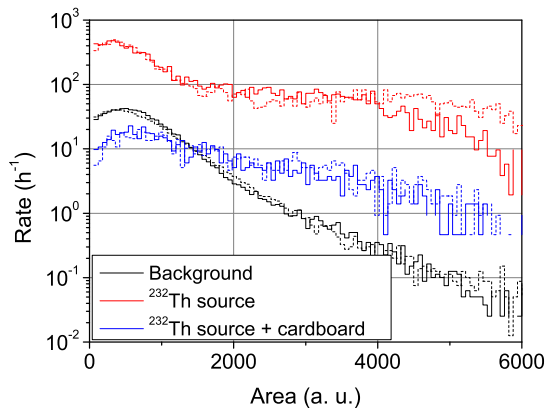


Figure 2: Distributions (per hour) of the area of each PMT signal in all the measurements performed without sample (see table 2): background measurement (black lines), measurement with ^{232}Th source (red lines) and with ^{232}Th source and a black cardboard between the PMTs (blue lines). Solid and dashed lines correspond to each one of the two PMT signals.

The distribution of this parameter depends on PMT gains, which were adjusted to give similar responses at a few per cent level.

These parameters have been calculated independently for each PMT signal, but when needed, they can be calculated for the sum pulse (in the case of the P1 parameter we will refer to this new parameter as P1s). In the following, we will study the distribution of these parameters and their correlations in the events registered for all the experimental runs summarized in table 2, after removing electronic noise (thanks to abnormal values of the maximum of digitized pulses) and applying some quality cuts (events showing baselines values out of range or negative areas due to analysis artifacts are also disregarded), as further described in section 3.2.

3.1. Measurements without sample

The measurements performed in our scintillation test bench without sample provided a population of PMT events. Figure 2 shows the distribution of the area of each PMT signal for the three measurements performed: without the external gamma source, with the source, and with the source and a black cardboard between the PMTs. A possible correlation between the two PMT signals has been studied by means of the Asy parameter, defined in eq. (2); distributions per hour of such a parameter are shown in figure 3 for the three measurements without sample.

The effect of gamma radiation on the PMTs is clearly evidenced by the comparison of the rates in the background measurement and with the ^{232}Th source,

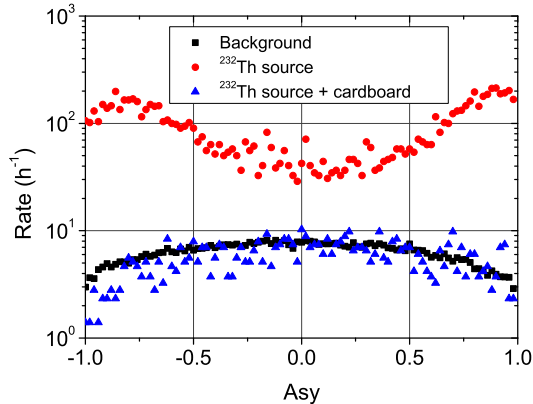


Figure 3: Distributions (per hour) of the Asy parameter in all the measurements performed without sample: background, with ^{232}Th source without black cardboard, and with ^{232}Th source and black cardboard.

both performed without sample. The trigger rate increased under gamma excitation by a factor ~ 14 , as shown in table 2; this increase is more important for events with larger areas (see figure 2). The gamma flux from the ^{232}Th source seems to generate a dominant population of strongly asymmetric coincident events, as shown in figure 3. To assess if this effect was related to the generation of light by the gamma quanta, the measurement with a black cardboard between the PMTs, preventing the light produced in one of them to reach the other one, was carried out. A clean sample of random coincidences has been obtained in this case (see figure 3). It can be observed in table 2 how the trigger rate is reduced a factor of 20 with respect to the measurement without cardboard (being this rate even lower than the one without the ^{232}Th source), confirming the effect of generation of light in a PMT being detected by the other one, described in [9]. Cherenkov light emission at PMT glass is possibly responsible for these events. Following figure 3, random coincidences could explain a large fraction of the events in the background measurement.

Pulse shapes digitized in all the measurements without sample are very similar. Figure 4 shows the average pulses of each PMT for random coincident events obtained in the measurement performed without sample, with ^{232}Th source and black cardboard. They show a gaussian shape with a 16 ns FWHM, in good agreement with PMT specifications.

Figure 5 presents the distributions of the parameters P1 and the number n of peaks identified per signal for the background measurement without sample. P1 is distributed around 0 as expected and the mean value of n is 2.71 and 1.54 for each one of the PMT signals. These distributions will be helpful to fix cut values in the event selection process implemented for the measurements with

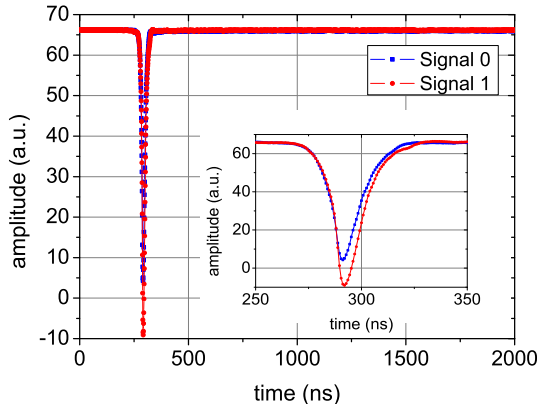


Figure 4: Average pulse shapes of each PMT signal for random coincident events obtained in the measurement performed without sample, with ^{232}Th source and black cardboard. The whole digitized window as well as a zoom are displayed.

samples, described in next section.

3.2. Measurements with samples

Once the events having their origin in the PMTs have been studied and characterized (see section 3.1), the measurements taken with the samples of natural quartz, synthetic quartz and methacrylate will be analyzed in this section. Figure 6 shows the distributions of the Asy parameter for the three materials and two measurements conditions; the same distributions in the measurements without sample (already shown in figure 3) are depicted also for comparison.

Following table 2, the trigger rate in background measurements is significantly higher than in the measurement without samples only for natural quartz, with an increase of about 30%. In the case of methacrylate, the rate is even reduced, reaching the same level than in the measurement with the black cardboard; it seems that the 10-cm thick methacrylate is somehow absorbing the light produced by PMTs (as shown in figure 6, symmetric events are particularly suppressed respect to the background measurement without sample). From the Asy distributions in the background measurements presented in figure 6, it is evident for natural quartz that a population of events having correlated PMT signals is present; the correlated signals have in addition large areas, as it can be seen in figure 7. For methacrylate and synthetic quartz there is not such an evidence of large area correlated events.

For the three samples the external gamma source produces an important increase in the trigger rates, comparing with the background conditions, of almost two orders of magnitude in the quartz samples and even higher for methacrylate

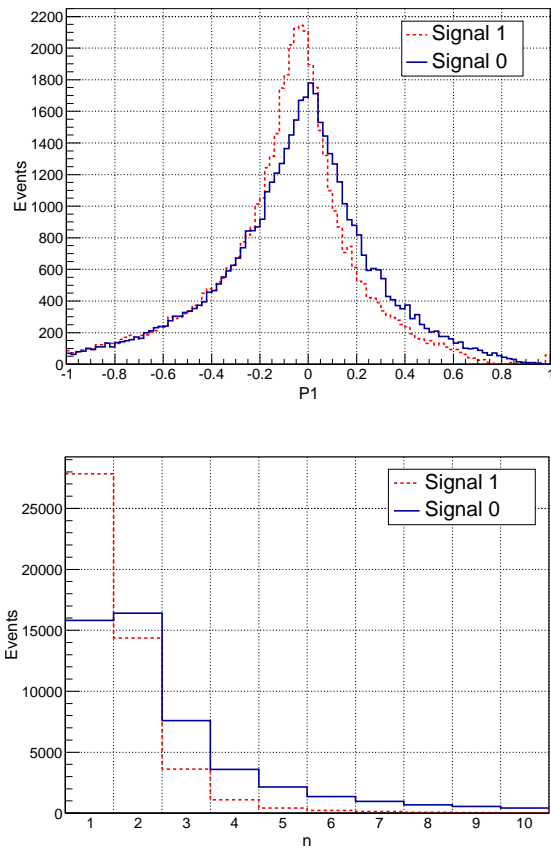


Figure 5: Distributions of parameters P_1 (top) and n (bottom) for the background measurement without sample. Distributions for signal 0 (blue solid lines) and 1 (red dashed lines) are independently shown.

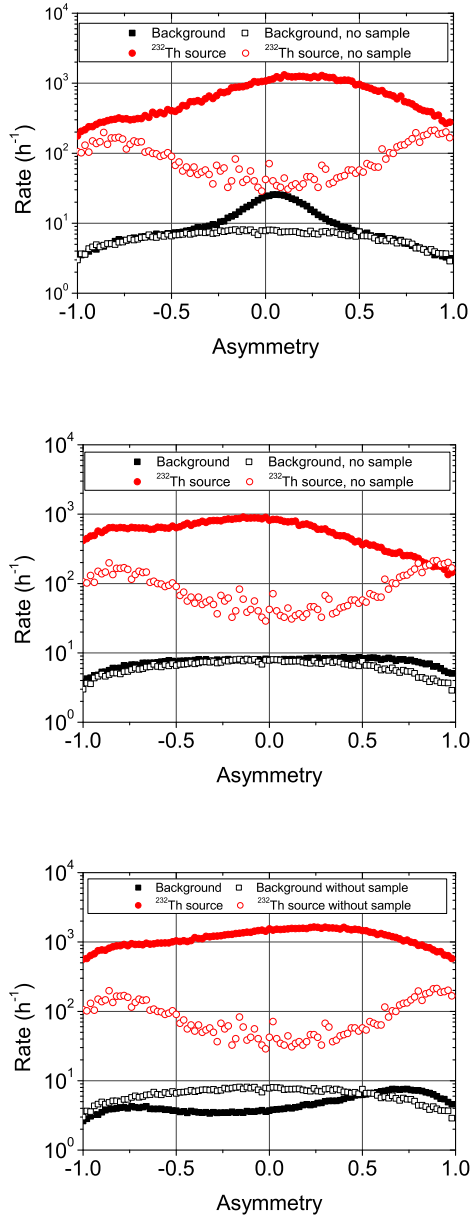


Figure 6: Distributions (per hour) of the Asy parameter in the measurements with natural quartz, synthetic quartz and methacrylate (from top to bottom). Results for background (in black squares) and under exposure to a ^{232}Th source (in red circles) are compared. Distributions corresponding to the measurements without sample shown in figure 3 are included also here for comparison (empty markers).

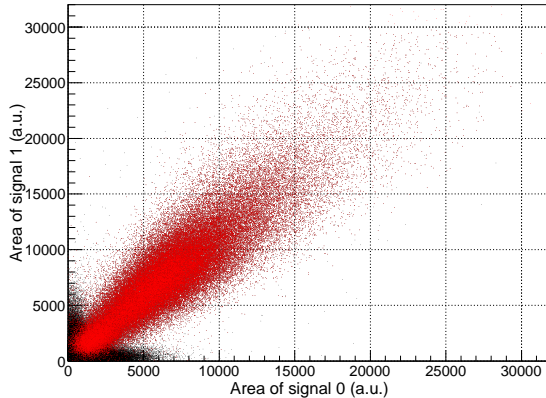


Figure 7: Correlation between the areas of each PMT signal for the natural quartz sample in the background measurement. Results before (in black) and after (in red) rejecting PMT-like events are shown.

(see table 2); following figure 6, the large amount of events generated under the gamma flux of the ^{232}Th source show a higher symmetry than those without the samples, pointing to some kind of light generation mechanism triggered by the gamma flux. Figure 8 compares the distributions of the sum area of the two PMT signals with the ^{232}Th source and in background conditions, for the three samples; the distribution for the measurement without sample and with the ^{232}Th is also included in all the plots in order to analyze the effect of the gamma flux on the sample. The rate increases due to the gamma flux in general for all the area range, but the bump that appears at high values (from 4000 to 8000 a.u.) seems to be mainly related to interactions in the PMTs rather than in the samples. However, for natural quartz the population of correlated events with very large areas (above 10000 a.u.) presents the same rate⁸.

In order to disentangle the events which could be attributed to scintillation in the samples from those just produced by PMTs, a selection process has been applied to the background and ^{232}Th measurements with the three samples and without sample. Results at different steps of this selection procedure are summarized in table 3. As mentioned before, electronic noise is first removed (step 1 in table 3) and quality cuts are then applied to reject events showing baselines values out of range or negative areas due to analysis artifacts (step 2 in table 3). Finally, events compatible with a PMT origin can be identified by counting the number n of peaks in the recorded pulses and also considering the P1 values [19] (step 3 in table 3). Figure 9 shows one of the PMT signals of three

⁸The low statistics in the measurement with the ^{232}Th source is due to the short time of data taking, in comparison with the background run.

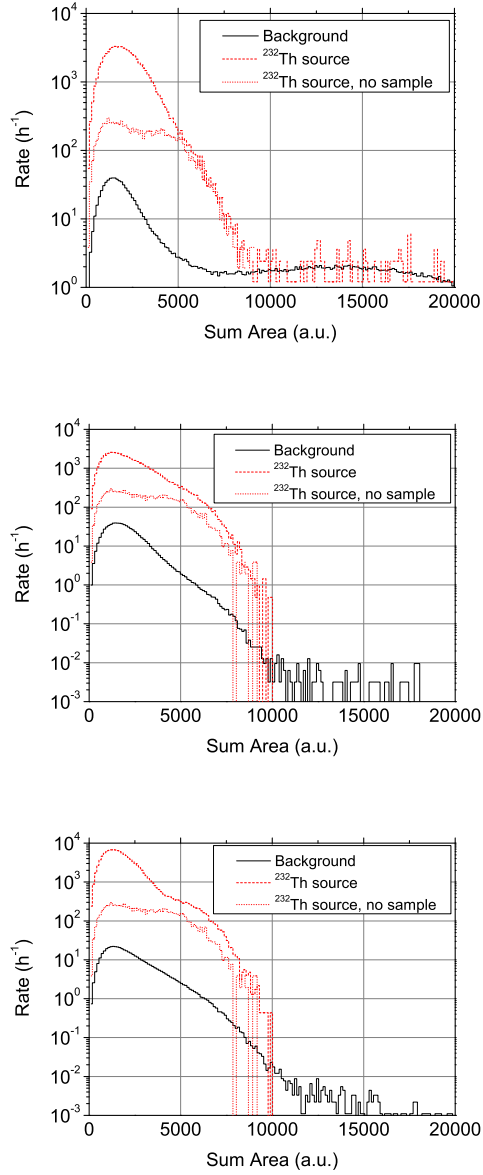


Figure 8: Distributions (per hour) of the sum area of the PMT signals in the measurements with natural quartz, synthetic quartz and methacrylate (from top to bottom). Results for background (black solid lines) and under exposure to a ²³²Th source (red dashed lines) are compared. The distribution obtained without sample and with the ²³²Th is also depicted in all the plots (red dotted lines).

Table 3: Counting rates (h^{-1}) at different steps of the selection process applied in the background measurements and with the ^{232}Th source for the three samples and without sample: 1) after removing electronic noise, 2) after applying quality cuts, 3) after filtering PMT-like events. The rate of identified PMT-like events corresponds to events in the step 2 minus those in step 3. Only statistical uncertainties are reported.

	Without sample	Natural quartz	Synthetic quartz	Methacrylate
Background				
1	920.9 ± 3.4	1217.2 ± 2.0	938.4 ± 1.7	615.5 ± 0.8
2	632.9 ± 2.8	979.5 ± 1.8	744.1 ± 1.5	468.1 ± 0.7
3	0.05 ± 0.03	302.6 ± 1.0	0.05 ± 0.01	0.08 ± 0.01
PMT-like events	632.9 ± 2.8	676.9 ± 2.0	744.1 ± 1.5	468.1 ± 0.7
^{232}Th source				
1	$(12.70 \pm 0.16) \times 10^3$	$(79.63 \pm 0.31) \times 10^3$	$(70.74 \pm 0.19) \times 10^3$	$(149.77 \pm 0.26) \times 10^3$
2	$(8.98 \pm 0.13) \times 10^3$	$(69.04 \pm 0.29) \times 10^3$	$(57.55 \pm 0.17) \times 10^3$	$(117.53 \pm 0.23) \times 10^3$
3	< 5.8 (95% C.L.)	237 ± 17	0.96 ± 0.68	0.44 ± 0.44
PMT-like events	$(8.98 \pm 0.13) \times 10^3$	$(68.80 \pm 0.29) \times 10^3$	$(57.55 \pm 0.17) \times 10^3$	$(117.53 \pm 0.23) \times 10^3$
^{232}Th source with black cardboard				
1	654 ± 17			
2	568 ± 16			
3	< 1.4 (95% C.L.)			
PMT-like events	568 ± 16			

example events chosen with very different n values, one obtained without sample and attributed to PMT origin (top) and the other two corresponding to the natural quartz background measurement (middle and bottom). In particular, values $n > 4$ and $P1 > 0.3$ at both PMT signals, derived from the distributions shown in figure 5, have been required for selecting non PMT-like events. The so-called PMT-like events include not only PMT noise but also any fast light emission in the samples, in the few ns range, which is indistinguishable from events having the origin directly in the PMT. Hence, it has to be stressed that only relatively slow scintillation events survive in the selection process applied and can be singled out by this method.

In the background measurements very few events remain after the filtering of PMT-like events, except for natural quartz: in this case, a population of events is singled out by the filtering, showing a rate almost four orders of magnitude higher than the corresponding to the other materials. This population can be attributed to scintillation in natural quartz, that will be below further analyzed. It is worth noting that according to table 3 the PMT-like events rate is of the same order in the four cases, which might be considered a confirmation of their common origin. In figure 7 the effect of the selection process on the correlation between the areas of each PMT signal is presented for the background measurement with the natural quartz sample; the surviving population

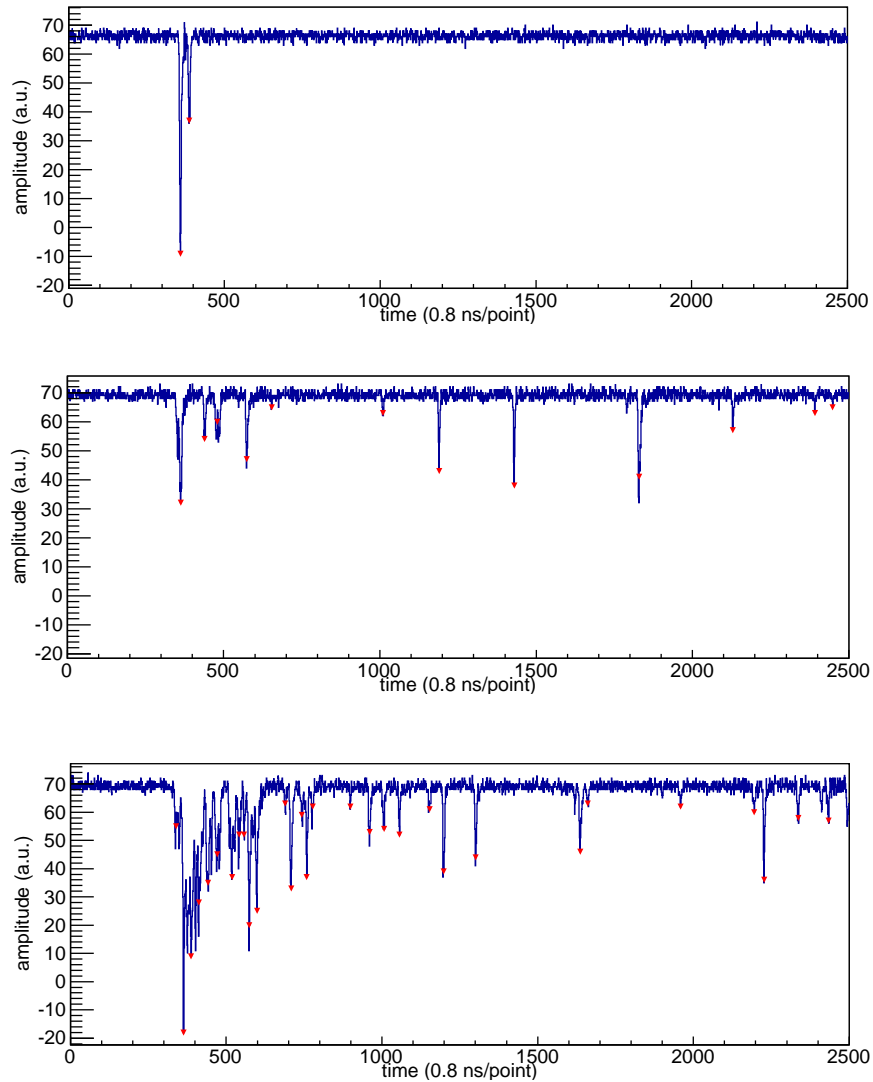


Figure 9: One of the PMT signals for a PMT-like event obtained in the measurement with ^{232}Th source and black cardboard (top) and for two events with low and high values of n from the background measurement with the natural quartz (middle and bottom). The peaks identified in the pulses are marked with triangles and counted to derive the n parameter.

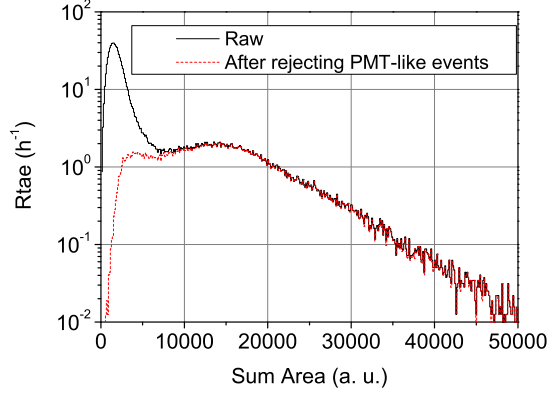


Figure 10: Distribution (per hour) of the sum of the areas for the natural quartz sample in the background measurement. Results before (black solid line) and after (red dashed line) rejecting PMT-like events are shown.

of large, symmetric events in natural quartz is clearly singled out. Distributions of the event areas summing the contributions from the two PMT signals, before and after applying the selection process, are presented also in figure 10 for the natural quartz in the background measurement; the region of large area events is unaffected.

Similar results are obtained when applying the described selection process also to the measurements performed with the ^{232}Th source. For the natural quartz sample 197 events remain, corresponding to a rate of $(237 \pm 17) \text{ h}^{-1}$. This rate is of same order, even lower, than the rate of $(302.6 \pm 1.0) \text{ h}^{-1}$ obtained in the background measurement, which indicates that the gamma excitation does not influence the population of scintillation events identified in natural quartz. This analysis should have produced more compatibility between both estimates of scintillation events; being this discrepancy an estimate of the possible systematic effects, very difficult to evaluate, in the application of the cuts (see table 3).

The presented results altogether confirm the existence for the natural quartz of a population of events having large and highly positively correlated areas in both PMT signals, with a number of peaks per event pulse and a P1 value which are not compatible with those of PMT-like events.

It has been already commented that for all the materials strong increase in rate is observed under gamma irradiation. Events contributing to this rate increase are indistinguishable from PMT noise, according to our analysis. These events could be explained by any prompt light generation mechanism, as for instance will be expected for the Cherenkov emission in quartz, methacrylate or even the PMT glass: corresponding energy threshold, timing properties and light yield expected [8] are roughly consistent with the observations. Since an

Table 4: Results of the two-gaussian fit (plotted in figure 11, bottom) of the distribution of the P1s parameter for the populations singled out in natural quartz.

	Population I	Population II
μ	0.5237 ± 0.0008	0.7404 ± 0.0008
σ	0.0711 ± 0.0008	0.0745 ± 0.0008
Area rate (h^{-1})	144.4 ± 1.5	157.8 ± 1.5

event-by-event selection of the populations induced by the gamma flux has not been possible, in next section we will focus in further understanding of the natural quartz scintillation.

3.3. Characterization of scintillation in natural quartz

The presence of two possible different populations of scintillation events in natural quartz with large and positively correlated areas is evidenced by analyzing the P1 parameter distribution for the two PMT signals, shown in figure 11, top. We will refer in the following to population I (II) as the one corresponding to faster (slower) events with the lower (higher) P1 values. A two-gaussian fit has been attempted for the P1s distribution, shown in figure 11, bottom; the fit parameters are summarized in table 4. The areas of each gaussian give the number of events assigned to each population, which are roughly half of the total number of non PMT-like events.

Pulse shapes are quite different for both populations. To consider the most representative events of each population, only events in the 1σ window around the mean value in the P1s distributions of figure 11, bottom, have been taken into account to derive mean pulses. Figure 12 presents these mean pulses as well as a typical individual pulse for populations I and II; the two PMT signals are well compatible and therefore have been averaged. This average pulse has been fit to a sum of exponential decay terms in order to deduce possible scintillation time constants:

$$V(t) = DC + A_{rise} \exp\left(-\frac{t-t_0}{\tau_{rise}}\right) - \sum A_i \exp\left(-\frac{t-t_0}{\tau_i}\right) \quad (3)$$

being DC the baseline value, t_0 the start time of the pulse, A_{rise} and τ_{rise} the amplitude and time constant of the rise component and A_i and τ_i those of the i-th decay term.

Figure 13, top presents the average pulse shape for population I events (already shown in figure 12) and the corresponding best fit found, using eq. (3) with one rise and two decay time constants. The results of the fit are summarized in table 5. The rise time constant is of the order of the one expected for the PMT model used while the decay time constants are in the typical range for inorganic scintillators; for example, for oxides with Si time constants reported in [11] range from some tens to some hundreds ns. The decay time constants found are fully compatible with those derived when fitting only the decay of the pulse to two exponential components.

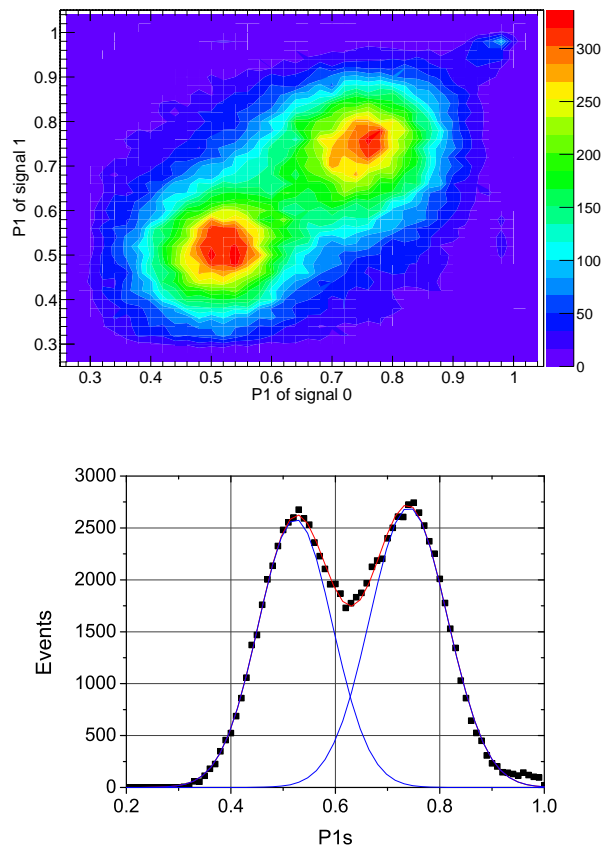


Figure 11: Correlation between the P1 values of the two PMT signals (top) and distribution of P1s parameter (bottom), for the events attributed to scintillation in the background measurement with natural quartz, after filtering PMT-like events. Two different populations can be distinguished, referred as population I (II) the one with the faster (slower) events. The fit to two gaussians of the P1s distribution is depicted in solid lines and results shown in table 4.

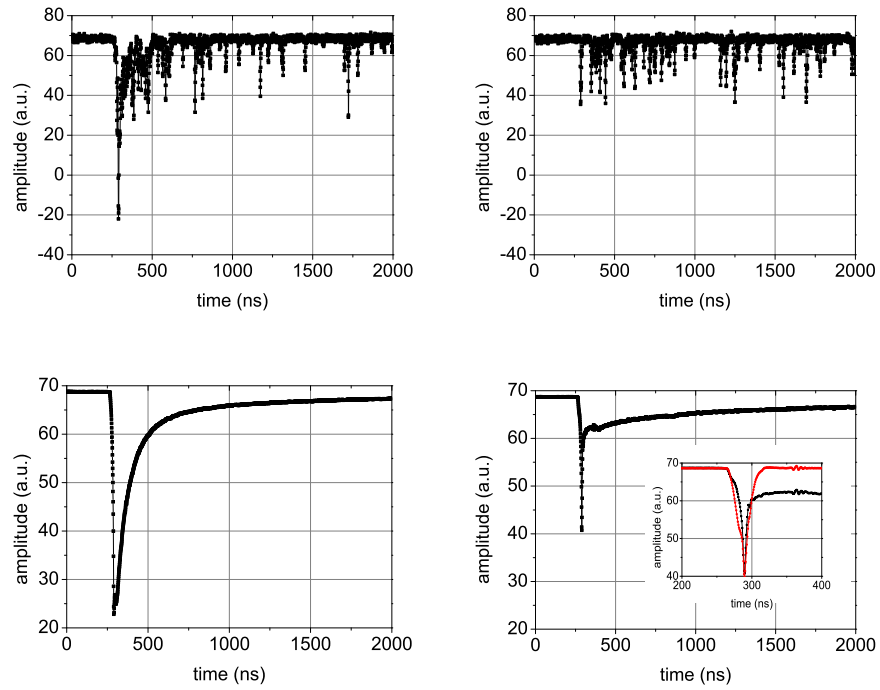


Figure 12: Examples of individual pulses (top) and the mean pulse shapes (bottom) derived for the population I (left) and population II (right) of scintillation events identified in natural quartz. Average of the two PMT signals have been considered for the building of the mean pulse shapes. The inset in the plot of the mean pulse of population II zooms the beginning of the pulse and shows the comparison with the mean pulse obtained for single photoelectrons (selected with $n=1$) in the background measurement without sample (red line).

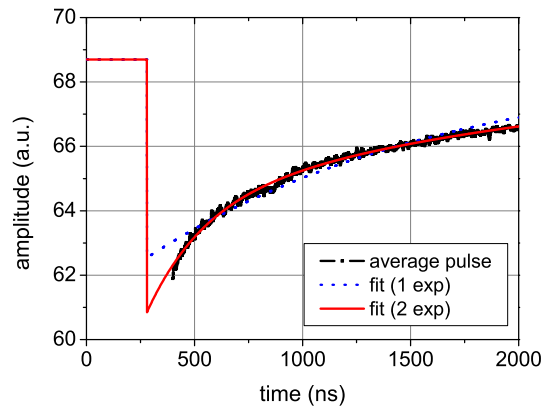
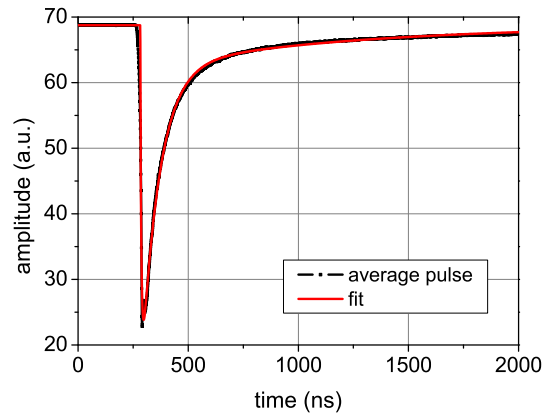


Figure 13: Average pulses (in black) and the corresponding fits to eq. (3) for scintillation events populations I (top) and II (bottom) identified in natural quartz; fits with two decay time constants (in red) or only one (in blue) are shown. Fit parameters are summarized in table 5.

Table 5: Results of the fits to eq. (3) of the average mean pulses shown in figure 13 for the two populations identified in natural quartz, considering different exponential terms: one rise and two decay constants for population I but only one or two decay constants for population II.

	Population I		Population II		Population II	
	A (a.u.)	τ (ns)	A (a.u.)	τ (μ s)	A (a.u.)	τ (μ s)
Rise	48 ± 49	5.0 ± 0.9	-	-	-	-
Decay 1	49.1 ± 3.6	81.1 ± 6.6	3.4 ± 2.9	0.27 ± 0.66	6.16 ± 0.59	1.40 ± 0.26
Decay 2	6.6 ± 1.2	932 ± 205	4.4 ± 4.7	2.3 ± 3.7	-	-
t_0 (ns)	283.0 ± 5.1		280.0 (fixed)		280.0 (fixed)	
DC (a.u.)	68.7 (fixed)		68.7 (fixed)		68.7 (fixed)	

As shown in figure 12, bottom right, the mean pulse for population II presents a strange behavior in the first nanoseconds range. A zoom of this region is shown in the inset of figure 12 and the mean pulse for population II is compared with the mean pulse corresponding to single photoelectrons (selected by choosing $n=1$ in the data from the background measurement without sample); the similarity between the two pulse shapes points to an artifact produced at the averaging by the fixed trigger position and strengthened by the low photon density registered in population II events. Therefore, only the decay part of the pulse, from 400 ns, has been considered in the fit. The best fits found for one or two decay time constants are shown in figure 13, bottom, and the results presented in table 5. The digitization window of 2μ s is showing just the beginning of a much longer signal, then our data cannot allow to derive the decay time constants precisely: the fit to only one exponential decay does not explain properly our observations (see figure 13, bottom), whereas the fit to two exponential decays is affected by strong uncertainties in the fit parameters (see table 5).

A rough estimation of the scintillation yield in the natural quartz can be attempted comparing the areas of the selected events for the two populations with those obtained without sample. Figure 14 shows the distributions of the sum area of the PMT signals relative to the mean sum area of pulses with $n=1$ in the background measurement without sample, which we assume is an estimate of the single photoelectron area. The deduced light yield is about 12 (11) photoelectrons for populations I (II), although in the latter only a fraction of the light emitted is registered because of the digitization window chosen.

3.4. Possible interpretation

Once the effect observed in natural quartz has been characterized, a possible explanation could be searched for. The first question to be addressed is why luminescent centers are present in the natural material while not in the synthetic one, and the second one, which particles or emissions are responsible for the excitation of these centers and the subsequent production of scintillation light.

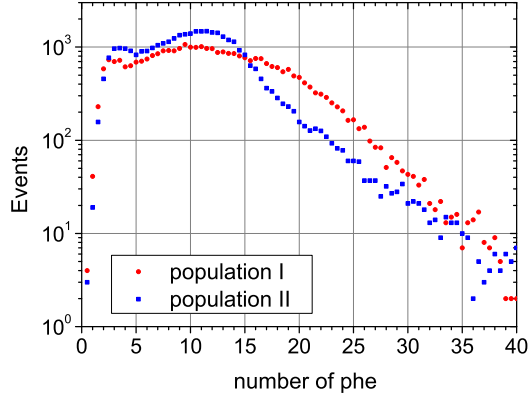


Figure 14: Distributions of the number of photoelectrons yielded for the populations I (red circles) and II (blue squares) identified in natural quartz, estimated as the sum area of the PMT signals relative to the mean sum area of pulses with $n=1$ in the background measurement without sample.

With respect to the first of the above proposed questions, in an inorganic solid, luminescent centers are typically due to substitutional impurities, excess atoms or ions and structure defects [10, 11]. For instance, metallic impurities are related to broken Si-O-Si bonds in quartz [20]. According to the chemical purity specifications given by the provider, the highest metallic impurities in the quartz samples measured are those of Al, with a value of 20 ppm for natural quartz and 0.1 ppm for synthetic quartz. On the other hand, natural quartz must have been more exposed to cosmic rays and environmental radioactivity than synthetic quartz, and radiation exposure can create defects in crystals (see for instance [11]).

Concerning the second question, although in principle, different particles could trigger the scintillation observed, we can discard gamma radiation and cosmic muons and only internal alpha contamination fulfills all the requirements:

- Environmental gamma radiation can be disregarded as the rate of events in the two identified populations has not increased when measuring with a ^{232}Th source, producing photons of different energies up to 2614.5 keV inside the lead shielding.
- Cosmic muons cannot be responsible since the reduced flux arriving at LSC cannot account for the rate of events measured for the natural quartz sample by more than three orders of magnitude.
- α particles generated by internal ^{232}Th and ^{238}U contamination in the sample, with energies from about 4 to 8 MeV, would be good candidates,

specially taking into account results in [12]. Assuming secular equilibrium in the chains and considering that each alpha particle emitted gives a scintillation event, an activity of 55 mBq/kg of ^{232}Th or 41 mBq/kg of ^{238}U would be necessary to justify the counting rate of scintillation events of 0.08 Hz measured for the two populations altogether. Comparing these values with the activities reported in table 1, the measured value of ^{238}U for natural quartz is larger than necessary, but it must be noted that faint scintillation events could have been lost in the PMT-like events rejection process and also it may be possible that only alpha particles with energy above a threshold produce a detectable effect. For synthetic quartz and methacrylate only upper limits to the activity of ^{232}Th and ^{238}U chains have been set, so the effect, even if not observed, cannot be excluded.

4. Conclusions

Possible scintillation in natural and synthetic quartz and methacrylate has been investigated at LSC, in a specially designed scintillation test bench using two PMTs in coincidence. Measurements have been carried out in low background environment as well as exposed to an intense gamma flux generated by a ^{232}Th source of about 5 kBq.

The important increase in counting rates and the more correlated signals registered by the two PMTs when exposing the materials to the gamma flux points to the production, in all the investigated samples, of a very fast light emission, which cannot be distinguished from the PMT noise in our study. Hence, this kind of events could be easily rejected when operating a detector with light guides or coupling windows made of these materials. This effect is probably due to the Cherenkov light emission by relativistic particles, like electrons, produced in quartz, methacrylate and PMT glass.

A different scintillation effect, observed in background conditions, has been evidenced in natural quartz and partially characterized. These events show large, highly correlated signals in both PMTs. Two distinct populations have indeed been identified; one of them has been fit to two exponential decays, obtaining values of the decay time constants of the order of those of inorganic materials ((81 ± 7) ns and (0.9 ± 0.2) μs , the latter with smaller amplitude) while the other population contains a slower component with a decay time constant of $\sim 1\text{-}2$ μs . This observed scintillation in natural quartz optical windows could produce events difficult to disentangle from scintillation at low energies, for instance, in NaI(Tl) detectors.

Although the origin of this scintillation has not been investigated (and indeed two mechanisms with different properties seem to be necessary to explain the two observed populations), the appearance of luminescence centers in natural quartz could be attributed to either impurities or to structural defects. Disregarded as origin of the scintillation gamma radiation and cosmic muons, the hypothesis of α particles from internal contaminations in the natural chains seems the most plausible.

5. Acknowledgements

This work has been supported by the Spanish Ministerio de Economía y Competitividad and the European Regional Development Fund (MINECO-FEDER) (grants FPA2008-03228, FPA2011-23749), the Consolider-Ingenio 2010 Programme under grants MULTIDARK CSD2009- 00064 and CPAN CSD2007-00042, and the Gobierno de Aragón (Group in Nuclear and Astroparticle Physics, ARAID Foundation and C. Cuesta predoctoral grant). C. Ginestra and P. Villar have been supported by the MINECO Subprograma de Formación de Personal Investigador. We also acknowledge LSC and GIFNA staff for their support.

References

- [1] S.R. Elliott, “Recent Progress in Double Beta Decay”, *Mod. Phys. Lett. A* 27 (2012) 1230009, and references therein.
- [2] L. Baudis, “Direct dark matter detection: The next decade”, *Physics of the Dark Universe* 1 (2012) 94-108, and references therein.
- [3] R. Bernabei et al, “Performances of the new high quantum efficiency PMTs in DAMA/LIBRA”, *JINST* 7 (2012) P03009.
- [4] K. Lung et al, “Characterization of the Hamamatsu R11410-10 3-in. photomultiplier tube for liquid xenon dark matter direct detection experiments”, *Nucl. Instrum. and Meth. A* 696 (2012) 32-39. L. Baudis et al, “Performance of the Hamamatsu R11410 Photomultiplier Tube in cryogenic Xenon Environments”, *JINST* 8 (2013) P04026.
- [5] J. Amaré et al, “Update on the ANAIS experiment. ANAIS-0 prototype results at the new Canfranc Underground Laboratory”, *J. Phys. (Conference Series)* 375 (2012) 012026. J. Amaré et al, “Preliminary results of ANAIS-25”, *Nucl. Instrum. Meth. A*, in press (2013).
- [6] S. Cebrián et al, “Background model for a NaI(Tl) detector devoted to dark matter searches”, *Astropart. Phys.* 37 (2012) 60.
- [7] C. Cuesta et al, “Slow scintillation time constants in NaI(Tl) for different interacting particles”, *Optical Materials* 36 (2013) 316-320.
- [8] G.F. Knoll, “Radiation Detection and Measurement”, (2000) John Wiley & Sons, Third Edition.
- [9] M. Robinson et al, “Reduction of coincident photomultiplier noise relevant to astroparticle physics experiments”, *Nucl. Instrum. and Meth. A* 545 (2005) 225-233.
- [10] J.B. Birks, “The theory and practice of scintillation counting”, (1964) Pergamon Press.

- [11] P. Lecoq, A. Annenkov, A. Gekhtin, M. Korzhik and C. Pedrini, “Inorganic Scintillators for Detector Systems: Physical Principles and Crystal Engineering”, (2006) Springer-Verlag.
- [12] J.B. Birks and J.W. King, “The luminescence of Air, Glass and Quartz under α -Particle Irradiation”, Proc. Phys. Soc LXVI (1953) 81-84.
- [13] M.J. Aitken, “Thermoluminescence Dating”, Academic Press, London (1985). M.J. Aitken, “Introduction to Optical Dating”, Oxford University Press (1998).
- [14] G. Luzón et al, “Characterization of the Canfranc Underground Laboratory”, Proceedings of the 6th International Workshop on the Identification of Dark Matter, (2007) World Scientific, p. 514-519.
- [15] A. Bettini, “Underground laboratories”, Nucl. Instrum. Meth. A 626-627 (2011) S64-S68.
- [16] R. Brun and F. Rademakers, “ROOT - An object oriented data analysis framework”, Nucl. Instrum. Meth. A 389 (1997) 81-86, <http://root.cern.ch>
- [17] R. Bernabei et al, “Performances of the \simeq 100 kg NaI(Tl) set-up of the DAMA experiment at Gran Sasso”, Il Nuovo Cimento A 112 issue 6 (1999) 545.
- [18] M. Morhac et al, “Identification of peaks in multidimensional coincidence-ray spectra”, Nucl. Instrum. Meth. A 443 (2000) 108-125.
- [19] C. Cuesta, “ANAIS-0: Feasibility study for a 250 kg NaI(Tl) dark matter search experiment at the Canfranc Underground Laboratory”, PhD thesis, University of Zaragoza, May 2013.
- [20] A. Deshkovskaya et al, “Spectral changes in Er⁺ and Tb⁺ -implanted fused silica”, Surface and Coatings Technology 158-159 (2002) 513-517.